DEPENDENCE ON FREQUENCY OF THE FAILURE PROCESS OF A SLOPE MADE UP OF COARSE PARTICLES

by
Kazuo KONAGAI[1] and Takeshi SATO[2]

1. INTRODUCTION

An irreversible deformation of a coarse particle assemblage is mainly due to change in its fabric. In order to observe the motion of interlocking particles, a new visualization technique (Laser-Aided Tomography: LAT) was developed by Konagai and Tamura[1),2)]. Using the LAT, Konagai, Tamura et al.[2)] and Hirata[3)] studied the dynamic response of an embankment model made up of coarse particles. The model was shaken sinusoidally on a shaking table with an amplitude of base acceleration being increased with time. The particles near the surface began to move when the amplitude of acceleration exceeded a threshold. Differing from the phenomena governed by the Coulomb's hypothesis, the threshold increased with increasing excitement frequency, and the bigger the representative grain size is, the clearer the tendency is. The result is consistent with the findings by Tamura et al[4)] through their experiments on models of fill dams. Since this phenomenon differs much from the one of a finer grain assemblage, it will be needed to be taken into account when dynamic stability of this kind of granular structure is discussed.

2. PROCESS OF FAILURE OBSERVED IN THE LAT EXPERIMENT

A new visualization technique called "Laser-Aided Tomography" (LAT), was developed for the study of the dynamic behavior of underwater granular structures[1),2)]. In this method, a granular structure model made of particles of crushed glass immersed in a liquid with the same refractive index, consequently, becomes invisible. An intense laser-light sheet (LLS) is then passed through the model illuminating the contours of all the particles on a cross-section optically cut by the LLS. Thus, scanning the model with LLS enables us to observe its whole-field deformation (Fig. 1).

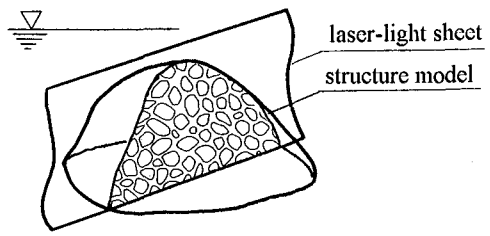

Fig. 1 Laser-Aided Tomography

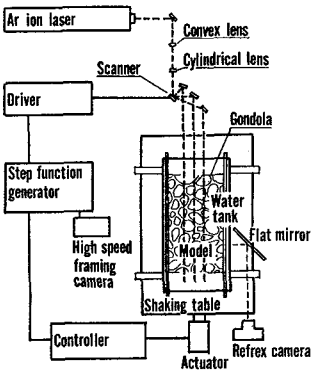

Fig. 2 Apparatus for dynamic failure test

---

[1]Associate Professor, Institute of Industrial Science, University of Tokyo.

[2]Graduate Student, ditto.

Dynamic failure tests of embankment-shaped models were conducted using the LAT. Coarse glass grains of two different sizes: fine (2 mm < grain < 5 mm) and medium (5 mm < grain < 12 mm) were piled up, within a gondola, into two embankment models with the same isosceles shape (height = 90 mm, slope = 1:2.72). The gondola was shaken sinusoidally within a water-tank full of liquid with the same refractive index (Fig. 2). The front and rear of the gondola were glazed, while both sides were open, and consequently, its motion did not stir the liquid much. A laser-light-sheet (LLS) traveled through the middle of the embankment's thickness. The amplitude of oscillation was increased linearly with time (6 gal/s). The embankment's surface began to slide when the base acceleration exceeded a threshold. Both Figs. 3(a) and 3(b) show the cross-section of the embankment model made up of smaller grains (2 mm < grain < 5 mm). These photographs were taken at (a) and (b) on Fig. 4, respectively. Fig. 4 shows variation of dilation of the right side of the embankment with base acceleration. Obviously, the surface failure of the embankment is accompanied by a considerable dilation.

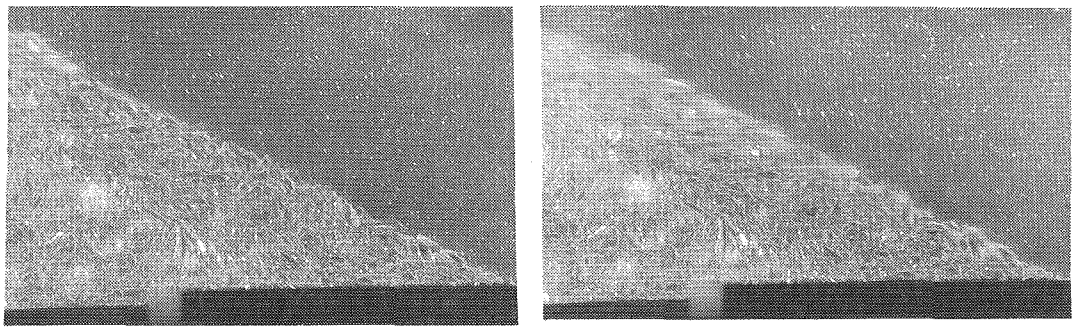

(a) *t=5s, acceleration=20gal* (b) *t=7s, acceleration=28gal*

Fig. 3 Cross-section of embankment model

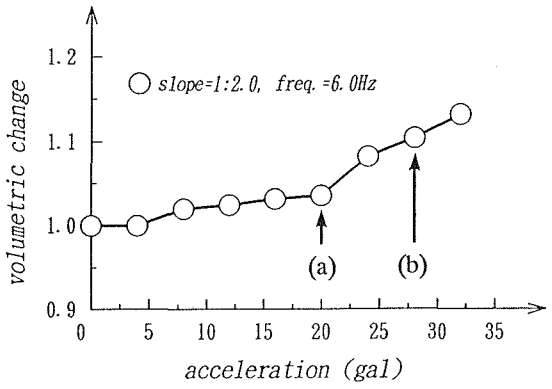

Fig. 4 Variation of $V_{dynamic} / V_{static}$ with acceleration

3. CONCEPTUAL MODEL OF SLOPE FAILURE

Taking into account the considerable dilation observed in the course of LAT experiments, a conceptual model of surface slide, shown in Fig. 5, is presented. In the model, a mass of particles, M, moves downward after being once lifted on a bumpy slip surface. During the process, some grains caught on the slip surface may roll with their surface rubbing against the surrounding grains, or these grains may scarcely rolled if they are embedded tightly. Given a specific material, either way, point o' on the bottom of the mass M will orbit the point o through an angle ϕ being attended by a energy loss through friction, and consequently, the model is governed by the following equations as:

$$M(\ddot{u}\cos\theta + \ddot{\phi}L\cos(\alpha-\phi)) = Mg\sin\theta - F_x \quad \text{....(1)}$$

$$M(\ddot{u}\sin\theta + \ddot{\phi}L\sin(\alpha-\phi)) = -Mg\cos\theta + F_z \quad \text{....(2)}$$

where, $\ddot{u}$ is an acceleration given to the model's base, L is the radial distance from the center of rotation o to o' on which the mass M is supported, and the L makes an angle $\alpha-\phi$ with the normal line to the slip surface with inclination of θ. Neglecting the inertia of the grain supporting the mass, contact forces F_x and F_z at point o' should satisfy the following equilibrium of moment around point o:

$$F_x \cdot L\cos(\alpha-\theta) \cong F_z \cdot L\sin(\alpha-\phi) + K_F Mg\mu L \quad \text{....(3)}$$

where, K_F shows the contribution of inter-particle friction to the process of surface sliding. Assuming that the acceleration component in the direction normal to the slip surface (left-hand side of eq.(2)) is negligibly small, and that sines and tangents of angles α, θ and ϕ can be approximated by their angles α, θ and ϕ, respectively, eq. (2) can be rewritten as:

$$\ddot{\phi} - \frac{g}{L}\phi = \frac{g}{L}(\theta - \alpha - K_F\mu - \frac{\ddot{u}}{g}) = -\frac{g}{L}(\frac{\ddot{u}}{g} + \theta_0 - \theta) \quad \text{....(4)}$$

If the inclination of the slope θ equals or exceeds $\alpha + K_F\mu$ in the above equation, no excitement is needed to slip the surface mass. In other words, $\alpha + K_F\mu$ here denotes the critical angle of slope θ_0. Let the given acceleration $\ddot{u}$ be:

$$\ddot{u} = -a\sin(\omega t + \chi) \quad \text{....(5)}$$

in which, χ is defined by the condition:

$$a\sin\chi = g\sin\alpha \quad \text{....(6)}$$

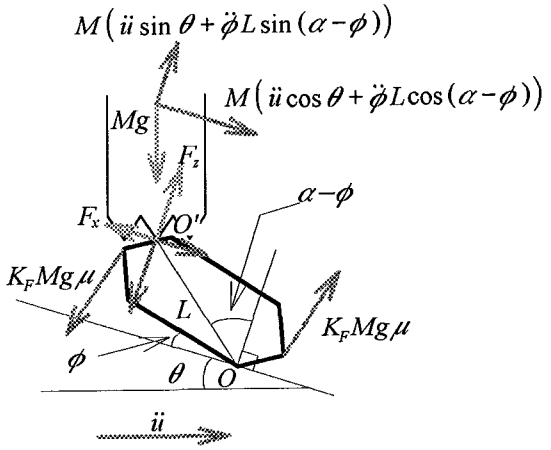

Fig.5 Conceptual Model of Surface Slide

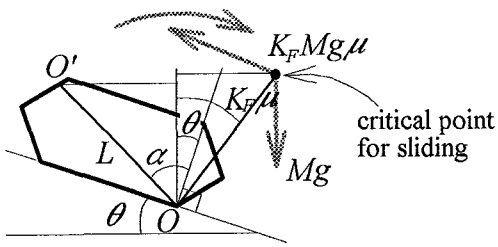

Fig.6 Rotation of a Particle

This insures that the base acceleration reaches the value required to initiate motion of the mass at time t=0. Substituting eqs. (5) and (6) in eq. (2) results in:

$$\ddot{\phi} - \frac{g}{L}\phi = \frac{g}{L}(\theta_0 - \theta)\left(\frac{\sin(\omega t + \chi)}{\sin\chi} - 1\right) \quad \text{....(7)}$$

This equation has the same form as the one for a rocking rectangular block does. Housner[5] solved it, and obtained a half-sine-wave acceleration pulse required for overturning a block. Picking up the procedures from Housner[5], a half-sine acceleration pulse required to initiate slip of the surface mass is obtained as:

$$a = g(\theta_0 - \theta)\sqrt{1 + \frac{L}{g}\omega^2} \quad \text{....(8)}$$

This implies that the failure acceleration a is a function of only four parameters; critical angle of slope θ_0, slope inclination θ, representative grain size L and excitement circular frequency ω.

For a large value of ω, eq. (8) can be represented by:

$$v = \frac{a}{\omega} \cong \sqrt{Lg}(\theta_0 - \theta) = \sqrt{Lg}(\alpha + K_F\mu - \theta) \quad \text{....(9)}$$

where, v is the maximum base velocity. Given the velocity v, the maximum kinetic energy K of the mass M is approximated by the following equation as:

$$\begin{aligned} K &= \frac{1}{2}Mv^2 = \frac{1}{2}MgL(\alpha - \theta)^2 + K_F\mu MgL(\alpha - \theta) + \frac{1}{2}MgL(K_F\mu)^2 \\ &= MgL\left(\frac{(\alpha - \theta)^2}{2} - \frac{(K_F\mu)^2}{2}\right) + K_F\mu MgL((\alpha - \theta) + K_F\mu) \\ &\cong MgL(\cos(K_F\mu) - \cos(\alpha - \theta)) + K_F\mu MgL(\alpha + (K_F\mu - \theta)) \\ &\cong \Delta U + \Delta W \end{aligned} \quad \text{...(10)}$$

where, ΔU and ΔW = increment of potential energy and energy loss through friction, respectively, required for the mass M to reach the critical point for slipping (Fig. 6).

When an assemblage of particles is put within a liquid, buoyancy and drag[6] from the liquid should be taken into account. Their effect on the failure acceleration is easily incorporated only by replacing gravitational acceleration g with g' which is defined as:

$$g' = \frac{\gamma_g - \gamma_w}{\gamma_g + C_m\gamma_w}g \quad \text{...(11)}$$

where, γ_g and γ_w are specific gravities of grain and liquid, respectively, and C_m is the added mass coefficient. The added mass coefficient should be determined by taking into account not only hydrodynamic pressure on a gently sloping surface of an embankment[6] but also grain-water-grain interaction. If the grain-water-grain interaction were negligibly small, many previous studies on drag force on a single grain would give us an idea how big the added mass coefficient is. Kotsubo and Takanishi[7], however, formulated disk-water-disk interaction, and showed that the added mass coefficient of a disk among the others is drastically changed if they are closely spaced. It may be one extreme approximation to add pore water mass directly to the grains' mass because the water trapped within the pore of a grain assemblage will move with the grains if particles are densely packed. In this case, the added mass coefficient C_m will be about the same as the void ratio, e. Concerning sand and gravel, void ratio, e, varies from 0.6 to 1.1, and consequently, the added mass coefficient C_m will lie within the same range. Whatever value the added mass coefficient is, g' is always smaller than g, and the failure acceleration should be smaller than the one by eq. (8). Not only that, frequency dependence of failure acceleration should be clearer.

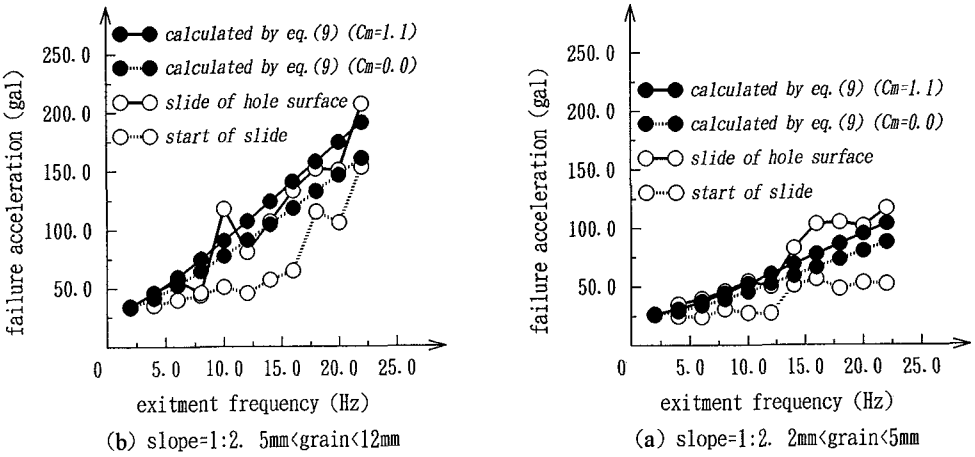

Fig. 7 Variation of failure acceleration with frequency

Figs. 7(a) and 7(b) show the variations with excitement frequency of failure acceleration of aforementioned two embankment models made up of smaller glass particles (2 mm < grain < 5 mm) and of bigger particles (5 mm < grain < 12 mm), respectively. In each figure, open circles connected by a broken line denote the accelerations required to initiate the surface slip (state like Fig. 3(a)), and those connected by a thick line show the accelerations at which the whole surface begins to slide (state like Fig 3(b)). On the other hand, solid circles show the failure accelerations calculated through eq. (8) assuming that the representative grain size L is the value in the middle of the grain size range. The value, $g(\theta_0 - \theta)$ in eq.(8), showing static threshold was set at 25 gal for the finer grains' assemblage, and 30 gal for the coarser grains' one. Since the biggest void ratio we can expect is about 1.1, the added mass coefficient C_m is expected to be smaller than this value. Thus, both two extreme cases (C_m=1.1 and C_m=0.0) are shown in each figure. The result, however, is not sensitive to the change in C_m. The acceleration given to the embankment base was not a half-sine pulse used to obtain eq. (8) but a continuously increasing sine wave. However, failure accelerations calculated through eq. (8) (solid circles) agree fairly well with the observed ones showing the thresholds of the whole surface failure, probably because its failure was triggered off by a sudden and considerable dilation as shown in Fig. 4. It should be noted that the base acceleration is usually smaller than the one at the top of an embankment. This will be the reason why the base acceleration required to initiate the surface failure is smaller than those by eq. (8).

Tamura, Okamoto and Kato[4] also indicated, through their experiments, that failure acceleration varies both with grain size and with excitement frequency. They conducted dynamic failure tests on models of fill dams on a large-scaled shaking table (length = 10 m, width = 2 m, height = 4 m). The following five materials were used to make up the models; (1) sandy silt, (2)river-bed gravel (L=2~100 mm), (3)angular gravel (L=5~10 mm), (4)roundish gravel (L=20~600 mm) and (5)coarse marble (L=100~300 mm). Fig. 8 shows variation of failure acceleration with grain size. Solid marks in this figure show calculated threshold acceleration using eq. (8) in which θ_0 is set at 43° picking up observed values in Ref. 4). As the acceleration becomes bigger, the observed threshold accelerations seem to become lower than the calculated values. Generally speaking, however, the bigger either the grain size or excitement frequency is, the bigger the threshold acceleration is, and this observed characteristic is consistent with the conceptual model's one.

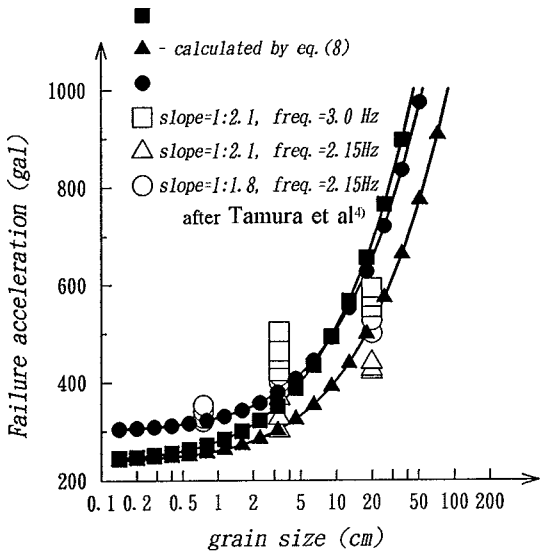

Fig. 8 Variation of failure acceleration with grain size

4. CONCLUSIONS

Failure process of a coarse particle assemblage is attended by a noticeable dilation which was observed through the new visualization technique, Laser-Aided Tomography (LAT). Taking into account the considerable dilation observed in the course of LAT experiments, a conceptual model of surface slide was presented. In the model, a mass of particles moves downward after being once lifted on a bumpy slip surface. According to the proposed model, a half-sine acceleration pulse required to initiate surface failure is given as a simple function of only four parameters; critical angle of slope θ_0, slope inclination θ, representative grain size L and excitement circular frequency ω. Variation of the failure acceleration either with grain size or with excitement frequency, observed through experiments, was consistent with the conceptual model's one, namely, the bigger either the grain size or excitement frequency is, the bigger the threshold acceleration is.

REFERENCES

1) Konagai, K. and C. Tamura: Visualization of Dynamic Change in Configuration of Underwater Particle Assemblage, Structural Dynamics, Krăzig et al. (eds.), Vol. 2, pp. 837-841, Balkema, Rotterdam, 1990.
2) Konagai, K., C. Tamura, P. Rangelow and T. Matsushima: Laser-Aided Tomography: A Tool for Visualization of Changes in the Fabric of Granular Assemblage, Structural Engineering / Earthquake Engineering, Vol. 9, No. 3, pp. 193s-201s, JSCE (Proc. of JSCE No. 455/I-21), 1992.
3) Hirata, K.: Fundamental Study on Dynamic Behavior of Embankment-shaped Granular Assemblage, Master Thesis, Univ. of Tokyo, 1990 (in Japanese).
4) Tamura, C., S. Okamoto and K. Kato: Dynamic Failure Tests on Rockfill Dam Models, "Tsuchi-to-Kiso", Japan Society of Soil Mechanics and Foundation Engineering, Vol. 20, No. 7, 1972 (in Japanese).
5) Housner, G.W.: The Behavior of Inverted Pendulum Structures During Earthquakes, Bull. of the Seismological Society of America, Vol. 53, No. 2, pp. 403-417, 1963.
6) Zanger, C.H.: Hydrodynamic Pressure on Dams due to Horizontal Earthquake Effects, U.S. Bureau of Reclamation, Engineering Monograph, No. 11, 1952.
7) Kotsubo, S. and T. Takanishi: A Method of Analysis of Dynamic Water Pressure during Earthquakes on Multi-Piles Foundation with Different Diameters and Arbitrary Position of Piles, Proc., JSCE, No. 276, pp. 1-12, 1978 (in Japanese).